Electronic states and luminescence in higher fullerene/porous Si nanocrystal composites

X. L. Wu[a] and Z. H. Deng
National Laboratory of Solid State Microstructures, Department of Physics, Nanjing University, Nanjing 210093, People's Republic of China

F. S. Xue
Nanjing Electronic Devices Institute, Nanjing 210016, People's Republic of China

G. G. Siu and Paul K. Chu
Department of Physics and Materials Science, City University of Hong Kong, Kowloon, Hong Kong, People's Republic of China

(Received 2 December 2005; accepted 13 April 2006; published online 7 June 2006)

Photoluminescence (PL) measurements have been performed on the nanocomposites of higher fullerene-coupled porous silicon (PS) nanocrystals. For the C_{70}/PS and $C_{76(78)}$/PS nanocomposites, the PL spectra show a pinning wavelength at ~565 nm and for the C_{84}/PS and C_{94}/PS nanosystems the pinning wavelength is at ~590 nm. The PL pinning property is closely related to the sorts of the coupled fullerenes. A band mixing model of direct and indirect gaps in a nanometer environment consisting of nc-Si core, SiO_2 surface layer, and coupled fullerene has been proposed for calculation of electronic states. Good agreement is achieved between the experiments and theory. © *2006 American Institute of Physics*. [DOI: 10.1063/1.2202742]

I. INTRODUCTION

An upsurge of research activities in the physics and applications of nanostructured materials has led to more attention to electronic states and luminescence properties of nanoparticle composites.[1–8] For typical luminescent nanomaterial, porous silicon (PS), many experiments have indicated that its luminescence property is not only determined by the quantum confinement effect of Si nanocrystals but also controlled by the surface chemical bonds.[3,6,7,9] Both the surface layer and nc-Si core constitute a nanoparticle composite. Naturally, its luminescence is a result of the interaction of the two nanoparticles. This kind of nanocomposite generally exists in luminescent semiconductor nanomaterials. Thus, study on electronic states of nanocomposites will be a precondition for understanding the luminescence mechanisms and improving the luminescence efficiency. However, the complexity of microscopic details and little theoretical research activities make the luminescent mechanisms of many nanocomposites still unclear or in controversy.

For fullerene molecules with highly symmetric structures and various unusual physical properties,[10] they have complicated electronic structures, but can only emit weak photoluminescence (PL) at low temperature. Under some experimental conditions, fullerene molecules can cluster and have different shapes and sizes.[11,12] To tailor their quantum confined sizes and nanometer environment for optimization of optical properties, the higher fullerene (C_{70}, $C_{76(78)}$, C_{84}, and C_{94})/PS nanocomposite is a suitable material for the investigation. In this Letter, we report the novel pinning behavior of the PL peak in fullerene/PS nanocomposites. We establish a band mixing model of direct and indirect gaps in a nanometer environment consisting of nc-Si core, SiO_2 surface layer, and coupled fullerene for calculation of electronic states. The consistency of the theory with experimental results clearly shows the validity of the band mixing model in explaining the luminescent features of nanoparticle composites.

II. SAMPLES AND EXPERIMENTS

Initial PS samples were prepared from ⟨100⟩-oriented *p*-type Si (~5 Ω cm) wafers by anodization in $C_2H_5OH:HF=1:2$ solution with a current density of 15–35 mA/cm^2. The PS layers with different porosities were obtained under an anodization time of 15–40 min. To form a nanocomposite of higher fullerene (C_{70}, $C_{76(78)}$, C_{84}, and C_{94}) with Si nanoparticles, as-made PS sample was chemically coupled with fullerene molecules through a coupling agent $[(CH_3O)_3Si(CH_2)_3NH_2]$. One end of the coupling agent is–NH_2, which easily combines with fullerene molecule by nucleophilic addition reaction, and the other end is–$Si(OCH_3)_3$, which has an affinity for hydrolysis-treated silicon. The coupling experiments have been described previously.[6] After the coupling for 24 h, the PL measurements were carried out at room temperature. The atomic force microscopy images from the coupling systems show the existence of fullerene cages with diameters of 15–20 nm,[13] indicating that the fullerene molecules have not been broken during the coupling.

[a]Author to whom correspondence should be addressed. Electronic mail: hkxlwu@nju.edu.cn

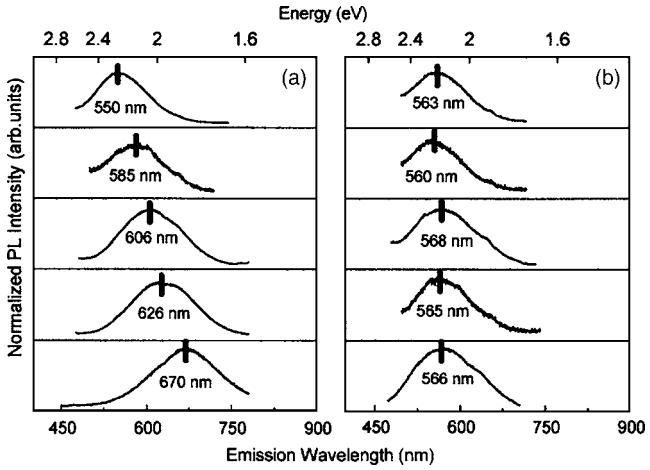

FIG. 1. PL spectra of a series of (a) as-made and (b) C_{70}-coupled PS nanocomposites.

III. RESULTS AND DISCUSSIONS

Figure 1(a) shows the PL spectra of a series of as-made PS samples taken from a Hitachi 820 fluorescence photospectrometer. After these samples were coupled with C_{70}, their PL intensities are generally reduced and their PL peak positions redshift or blueshift to a pinning wavelength at ~565 nm, as shown in Fig. 1(b). This result suggests that the pinning wavelength is not related to the sizes of original PS nanocrystals. The same pinning wavelength can be observed for the $C_{76(78)}$/PS nanocomposites. Figure 2(a) shows the PL spectra of two same PS samples coupled with C_{70} and $C_{76(78)}$, respectively. Obviously, they have a same pinning wavelength at ~565 nm, indicating that C_{70} and $C_{76(78)}$ have almost identical effect on the electronic states of PS nanocrystals.

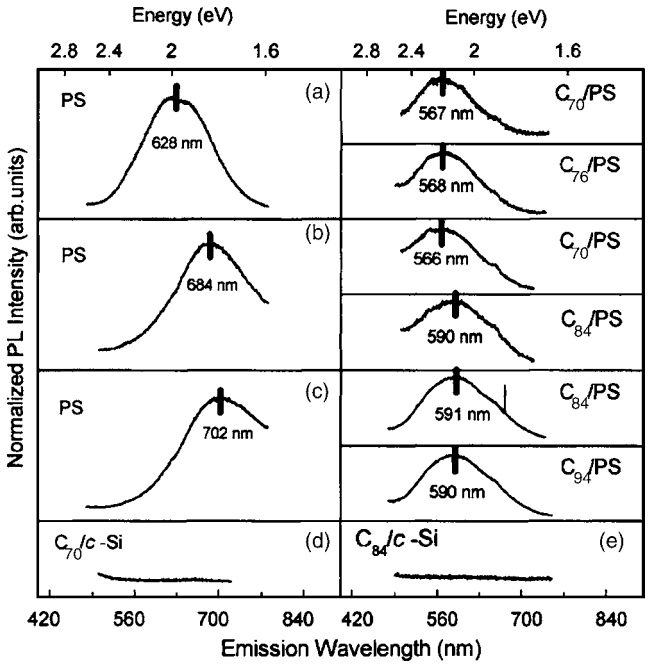

FIG. 2. (a)–(c) PL spectra of three as-made PS samples before and after the coupling with C_{70}, $C_{76(78)}$, C_{84}, and C_{94}. (d) and (e) PL spectra of the C_{70}- and C_{84}-coupled *c*-Si wafers, respectively.

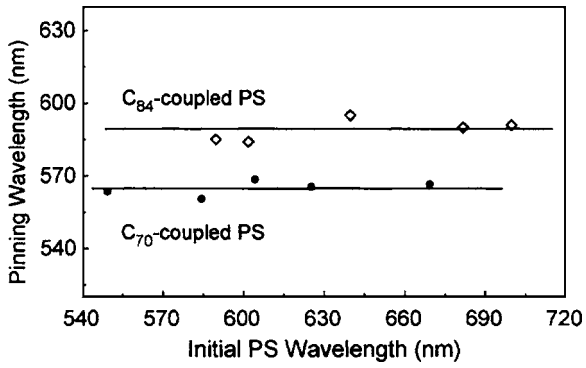

FIG. 3. PL spectral peak positions of a series of as-made PS samples vs those of the C_{84}-coupled PS samples. For comparison, similar result has also been given for the case of the C_{70}-coupled PS samples.

Figure 3 shows the PL spectral peak positions of a series of as-made PS samples versus those of the C_{84}-coupled PS samples. For comparison, similar result has also been given for the case of the C_{70}-coupled PS samples. We can see that a new pinning wavelength appears at ~590 nm for the C_{84}-coupled PS samples. In addition, we found that the PL intensities obviously decrease in the coupling samples. For the C_{94}-coupled PS nanocomposites, the pinning wavelength is still at ~590 nm. If a PS sample is cut into two pieces and they are, respectively, coupled with C_{70} and C_{84}, the PL spectra show different pinning wavelengths. The former is at ~565 nm and the latter at ~590 nm, as shown in Fig. 2(b). Further, if two same PS samples are coupled with C_{84} and C_{94}, the PL spectra show a same pinning wavelength at ~590 nm [see Fig. 2(c)]. The above results indicate that the electronic state feature of both C_{84} and C_{94} is similar but different from those of both C_{70} and $C_{76(78)}$.

Since no PL peak was observed in the fullerene-coupled single crystal Si wafers [Figs. 2(d) and 2(e)], the formation of the pinning wavelengths should relate to the fullerene/PS nanocomposite. To identify the luminescent origins, the PL excitation (PLE) spectra of these nanocomposites were examined and two typical PLE spectra are presented in the

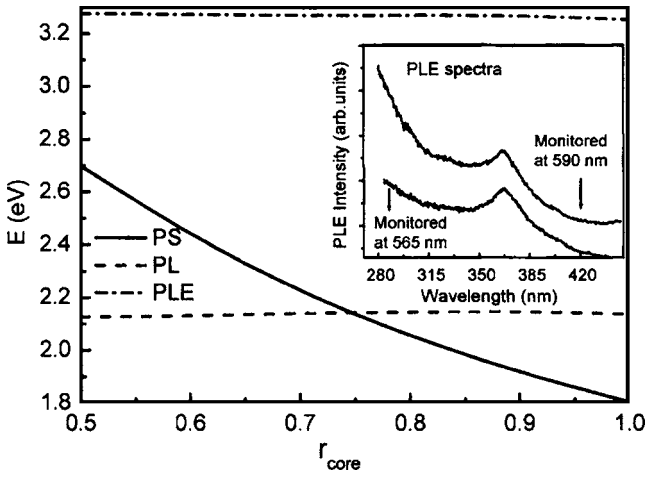

FIG. 4. PL (dash line) and PLE (dash dot line) transition energies as a function of the radius of Si core. The solid line shows the PL transition energies in PS. The inset shows the PLE spectra of the C_{70}/PS and C_{84}/PS nanocomposites taken under two different monitoring wavelengths.

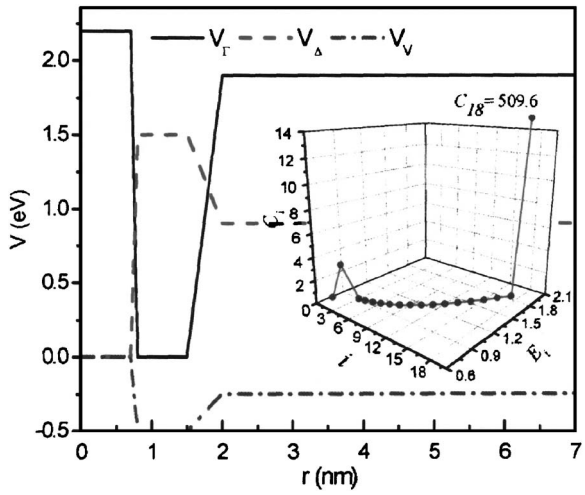

FIG. 5. Band structure of the nanocomposite consisting of indirect Si core, direct oxide layer, and higher fullerene. The solid, dash, and dash dot lines illustrate the Γ and Δ valleys in the conduction and valence bands. The energies in two transition regions are assumed to vary linearly with the core radius. The inset shows the calculated energy levels and their *C* coefficients.

inset of Fig. 4. We can see that an obvious PLE peak appears at ~370 nm under two different monitoring wavelengths. The PLE peak remains unchanged with the sorts of fullerenes, indicating that the absorption process of photoexcited carriers is the same in all the nanocomposites. The PLE peak was frequently observed in the PS samples,[14–16] but no exact explanation has been given for its origin so far. For our current nanocomposites, fullerene introduction into the surface of PS should not lead to a reduction of Si crystallite sizes but change the surface structure. However, we found that all the nanocomposites show almost identical Fourier-transform infrared absorption spectra.[6] Thus, the difference in pinning wavelength cannot be explained on the basis of the change of the PS surface structure. Previously, it has been proposed that the Si═O bond at the surface of PS nanocrystal be responsible for the 590 nm pinning wavelength in the naturally oxidized PS.[3] However, more theoretical calculations indicate that other oxygen-related bonding structures at the surface of small Si nanocrystal can also lead to similar result.[17–20] Currently, the explanation based on the Si═O binding state may not be suitable for elucidating the pinning behavior of the current PL peak, because the results of Fig. 2 have clearly shown that the pinning wavelength is dependent upon the sorts of the fullerenes. Since the fullerenes themselves do not show any PL, the PL pinning behavior should be considered to be a result of the interaction between the electronic states of three kinds of nanoparticles (nc-Si core, the surface layer, and higher fullerene). Below we adopt a band mixing model to explain very well the origins of both the observed pinning wavelength and the 370 nm PLE peak.[7,8,21,22]

In view of the inefficient PL feature of fullerene, its band may be inferred to be indirect. Hence the band structure of the nanocomposite consists of indirect Si core, direct oxide layer, and the coupled fullerene, as shown in Fig. 5, where the solid, dash, and dash dot lines illustrate the Γ and Δ valleys in the conduction band and valence band, respectively. The energies in two transition regions are assumed to be linear with distance. The Schrödinger equation may be written as[7]

$$\begin{pmatrix} H_\Gamma & H_{\Gamma\Delta} \\ H_{\Delta\Gamma} & H_\Delta \end{pmatrix} \begin{pmatrix} \Psi_\Gamma \\ \Psi_\Delta \end{pmatrix} = E \begin{pmatrix} \Psi_\Gamma \\ \Psi_\Delta \end{pmatrix},$$

where ψ_Γ and ψ_Δ are the wave functions for Γ and Δ valleys, respectively. In cylinder coordinate, the Hamiltonian is described as follows:

$$\begin{pmatrix} -\frac{\hbar^2}{2m_\Gamma}\left[\frac{1}{r}\frac{\partial}{\partial r}\left(r\frac{\partial}{\partial r}\right)+\frac{1}{r^2}\frac{\partial^2}{\partial\theta^2}+\frac{\partial^2}{\partial z^2}\right]+V_\Gamma & V_{\Gamma\Delta} \\ V_{\Delta\Gamma} & -\frac{\hbar^2}{2m_\Delta}\left[\frac{1}{r}\frac{\partial}{\partial r}\left(r\frac{\partial}{\partial r}\right)+\frac{1}{r^2}\frac{\partial^2}{\partial\theta^2}+\frac{\partial^2}{\partial z^2}\right]+V_\Delta \end{pmatrix},$$

where m_Γ and m_Δ are the effective masses at Γ and Δ valleys, V_Γ and V_Δ the potential energies for Γ and Δ wave functions, and $V_{\Gamma\Delta}$ and $V_{\Delta\Gamma}$ the coupling potentials between Γ and Δ energy valleys, respectively. Using the finite-difference method,[22] we can solve above Schrödinger equation and thus obtain the confined band mixing energy levels. A coupling coefficient *C* defined as the amplitude ratio of the Γ to Δ waves is introduced to characterize the state attribution. The inset of Fig. 5 shows the calculated energy levels and their *C* coefficients. Since the width of the coupled fullerene is rather large, crowded states appear above the Δ valley of the fullerene and the nanocomposite shows a bulk-like behavior. Most states are confined in the fullerene and their coupling coefficients are very small. Only the E_2 level has large C_2=3.26, showing a strong Γ-Δ mixing. Corresponding wave function is shown in Fig. 6, where the solid and dash lines stand for the Γ and Δ waves, respectively. The Ψ_Γ and Ψ_Δ are confined in oxide layer and Si core, respectively, just like the case in PS. We can expect the direct transition between E_2 and the confined state in valence band to produce the PL. Since the wave function of valence level is confined in the fullerene, different locations of wave peaks for electron and hole make the PL weaker than that in PS. However, we may see that E_{18}=1.908 eV is larger than the Γ

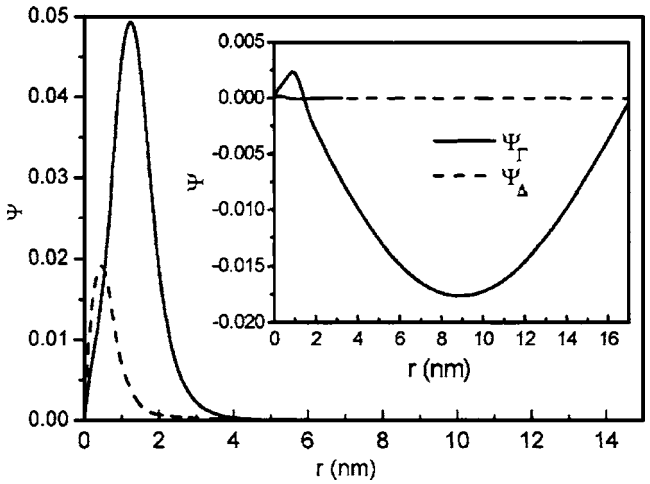

FIG. 6. Wave functions of the excited state E_2. The solid and dash lines stand for the Γ and Δ waves, respectively. The inset shows the wave functions of the excited state E_{18}. The Γ wave has extended into the coupling layer.

barrier in the fullerene and thus a strong Γ wave exists in the fullerene, as shown in the inset of Fig. 6. It is the strong Γ state that produces the strong absorption in our PLE spectra.

The PL and PLE transition energies calculated according to this band mixing model as a function of the radius of Si core are shown in Fig. 4 (dash and dash dotlines, respectively). Corresponding PL transition energies in PS shown by solid line are also included for comparison. The electron states in PS are confined in the Si core and oxide layer, and so its energy decreases with increasing the radius of Si core.[7] Within the radius range shown in Fig. 4, the PL wavelengths range from 460 to 690 nm. Although the wave function of the strong band mixing level E_2 in the fullerene/PS nanocomposite is also confined in Si core and oxide layer, its energy is determined by the wide fullerene Δ well. With increasing the radius of Si core, E_2 is locked in the range of 0.76–0.79 eV. Corresponding hole level is also decided by the wide Δ well in the fullerene, resulting in the 2.14 eV transition energy as shown in Fig. 4. The E_{18} level is locked at 1.908 eV for all radii of Si cores. The transition wavelength from E_{18} to valence band level may be calculated to be 379 nm, which is close to the observed PLE peak position. Taking different band offset for the C_{70}/PS and C_{84}/PS composites, we found with this calculation that the PL pinning behavior is different, exhibiting a different pinning wavelength. This is the cause for different fullerene-coupled PS samples to have different pinning wavelength. From our experimental results, we can infer that the band offset for the C_{70}/PS and $C_{76(78)}$/PS composites should be identical, but it is different from that for the C_{84}/PS and C_{94}/PS composites. This indicates that the electronic state characteristics of $C_{70}(C_{76(78)})$ are different from that of $C_{84}(C_{94})$.

IV. CONCLUSION

An interesting interaction between quantum confined and band mixing effects exists in nanocomposite, which makes PS luminous. When the PS is coupled with a large fullerene, the Γ and Δ waves will permeate into fullerene. Crowded states appear above the Δ valley of the fullerene and the nanocomposite shows a bulklike behavior. Since only a narrow direct gap oxide layer exists between large indirect gap Si core and the fullerene, only one strong band mixing state responsible for the PL transition occurs. The energy of the state is determined by the band mixing in nanocomposite and independent of the radius of Si core. This makes the PL wavelength pinned. The direct absorption edge of fullerene determines the PLE wavelength. Although the quantum confinement is weakened and some bulklike features appear during the coupling, the strong band mixing in some state is possible to make the nanocomposites luminous and lock the luminescent wavelength. Therefore, this sort of coupling opens a new way to tailor quantum confined sizes and nanometer environment for optimization of luminant properties.

ACKNOWLEDGMENTS

This work was supported by the Grant Nos. 10225416, 60476038, and 60576061 from the National Natural Science Foundation of China and the LAPEM. Partial support was also from the Major State Basic Research Project No.G001CB3095 of China and City University of Hong Kong Direct Allocation Grant No.9360110.

[1] *Condensed-Matter and Materials Physics*, edited by Committee on Condensed-Matter and Materials Physics Board on Physics and Astronomy (National Academy Press, Washington, DC, 1999).
[2] A. G. Cullis, L. T. Canham, and P. D. Calcott, J. Appl. Phys. **82**, 909 (1997).
[3] M. V. Wolkin, J. Jorne, P. M. Fauchet, G. Allan, and C. Delerue, Phys. Rev. Lett. **82**, 197 (1999).
[4] Y. Kanemitsu, H. Uto, and Y. Masumoto, Phys. Rev. B **48**, 2827 (1993).
[5] K. Koch and V. Petrova-Koch, *Porous Silicon*, edited by Z. C. Feng and R. Tsu (World Scientific, Singapore, 1994).
[6] X. L. Wu, S. J. Xiong, D. L. Fan, Y. Gu, X. M. Bao, G. G. Siu, and M. Stokes, Phys. Rev. B **62**, R7759 (2000).
[7] F. S. Xue, X. M. Bao, and F. Yan, J. Appl. Phys. **81**, 3175 (1997).
[8] X. L. Wu and F. S. Xue, Appl. Phys. Lett. **84**, 2808 (2004).
[9] J. L. Gole, F. P. Dudel, D. Grantier, and D. A. Dixon, Phys. Rev. B **56**, 2137 (1997).
[10] H. W. Kroto, J. R. Heath, S. C. Brien, R. F. Curl, and R. E. Smalley, Nature (London) **318**, 318 (1985).
[11] X. L. Wu, Y. Gu, S. J. Xiong, J. M. Zhu, G. S. Huang, B. X. Bao, and G. G. Siu, J. Appl. Phys. **94**, 5247 (2003).
[12] T. Qiu, X. L. Wu, C. X. Wu, X. Yang, X. F. Shao, G. S. Huang, and G. G. Siu, Appl. Phys. A: Mater. Sci. Process. **81**, 35 (2005).
[13] X. L. Wu, Y. Gu, S. J. Xiong, J. M. Zhu, G. S. Huang, B. X. Bao, and G. G. Siu, J. Appl. Phys. **94**, 5247 (2003).
[14] Y. H. Xie, W. L. Wilson, F. M. Ross, J. A. Mucha, E. A. Fitzgerald, J. M. Macaulay, and T. D. Harris, J. Appl. Phys. **71**, 2403 (1992).
[15] X. Q. Zheng, C. E. Liu, X. M. Bao, F. Yan, H. C. Yang, H. C. Chen, and X. L. Zheng, Solid State Commun. **87**, 1005 (1993).
[16] S. S. Deng, X. L. Wu, Z. Y. Zhang, Y. F. Mei, Y. Yang, H. Chen, and X. M. Bao, Phys. Lett. A **299**, 299 (2003).
[17] A. Puzder, A. J. Williamson, J. C. Grossman, and G. Galli, Phys. Rev. Lett. **88**, 097401 (2002).
[18] C. S. Garoufalis, D. Zdetsis, and S. Grimme, Phys. Rev. Lett. **87**, 276402 (2001).
[19] I. Vasiliev, J. R. Chelikowsky, and R. M. Martin, Phys. Rev. B **65**, 121302 (2002).
[20] F. Zhou and J. D. Head, J. Phys. Chem. B **104**, 9981 (2000).
[21] G. D. Sanders and Y. C. Chang, Phys. Rev. B **45**, 9202 (1992).
[22] S. L. Chuang and C. S. Chang, Semicond. Sci. Technol. **12**, 252 (1997).